

Electron Impact Ionization Cross-Section Maxima of Atoms

Antônio Carlos Fontes dos Santos ^{1,*}  and Károly Tókési ^{2,*} ¹ Physics Institute, Federal University Rio de Janeiro, Rio de Janeiro 21941-972, Brazil² Institute for Nuclear Research, (ATOMKI), 4026 Debrecen, Hungary

* Correspondence: toni@if.ufrj.br (A.C.F.d.S.); tokesi@atomki.hu (K.T.)

Abstract: Using measured cross-sections and polarizability data, an empirical scaling law is extracted for the electron collision single-ionization cross-section maxima of neutral atoms. We found that the cross sections scale linearly with the target's static polarizability. We confirm this observation using our present three-body classical trajectory Monte Carlo simulations.

Keywords: ionization cross sections; polarizability; classical trajectory Monte Carlo model

1. Introduction

The electron impact ionization of atoms has been studied for decades to interpret the underlying atomic processes [1–11]. Ionization by electrons has also been achieved, both experimentally and theoretically, to provide parameters for use in plasma physics, astrophysics, and gas discharge, to name a few. One can find large amounts of information in the literature, but the various pieces of data cannot be explored to deduce any regime and have been used only in limited systems.

A benchmark study on electron–atom interactions was conducted by Bethe (1930) [9], who established the well-known $\ln v^2/v^2$ expression of ionization cross-sections for high-speed collisions. Here, v is the speed of the electron. After the pioneering work of Bethe, considerable classical, empirical, and semi-empirical models have been suggested to interpret the ionization of matter by electrons. For instance, Otvos and Stevenson [10] showed that the maximum total ionization cross-sections for several neutral atoms and molecules are equal to the weighted contributions from the valence shell electrons. The authors observed that the weights were the mean square radii of each shell. More recently, Maiorov and Golyatina [11] presented an analysis of elastic and inelastic cross-sections of electrons with several atoms. Their formulas reproduce the values of the ionization cross-sections for hydrogen, metal, and other elements in a wide range of energies, with accurate orders of errors of the available theoretical and experimental data. In addition, these models are only useful within a narrow range of electron speed and/or target species. Several ab initio calculations have also been performed, although they are lengthy.

In the early 1960s, a new type of classical simulation was established. It is called the classical trajectory Monte Carlo method (CTMC). It was quite surprising that the classical description could accurately reproduce much experimental data. In general, the CTMC method is a non-perturbative method through which many-body interactions, or reaction channels, can be studied simultaneously, which is one of the advantages of the CTMC model [12]. The model can also handle multielectron systems where, in addition to the active target electron, it handles the effects of the other electrons.

The empirical scaling presented in this paper can be useful, for instance, for calibrating ion gauges [13] or for guiding theoretical studies of the ionization of multielectron systems via electron impact, by indicating what parameters are relevant. In addition, it can also be useful for evaluating the reliability of experimental data.

In order to investigate the dependence of the electron impact single-ionization cross-section maxima of neutral atomic species on the target properties, in the present work,



Citation: dos Santos, A.C.F.; Tókési, K. Electron Impact Ionization Cross-Section Maxima of Atoms. *Atoms* **2023**, *11*, 81. <https://doi.org/10.3390/atoms11050081>

Academic Editors: Giuseppe Mandaglio and Yew Kam Ho

Received: 15 February 2023

Revised: 1 May 2023

Accepted: 5 May 2023

Published: 8 May 2023



Copyright: © 2023 by the authors. Licensee MDPI, Basel, Switzerland. This article is an open access article distributed under the terms and conditions of the Creative Commons Attribution (CC BY) license (<https://creativecommons.org/licenses/by/4.0/>).

we determine the linear dependence of the single-ionization cross-section on the target polarizability. The experimental cross-sections and target polarizabilities for various atomic systems were obtained from the literature. We justify our observation using our three-body CTMC calculations.

2. Theory

To mimic experimental observation, we performed classical trajectory Monte Carlo calculations. In recent decades, there has been a great revival of the classical trajectory Monte Carlo (CTMC) calculations applied in atomic collisions involving three or more particles [12]. This approximation seems to be useful in treating atomic collisions where the quantum mechanical ones become very complicated or unfeasible. This is usually the case when higher-order perturbations should be applied, or when many particles take part in the processes.

One of the advantages of the CTMC method is that many-body interactions are precisely considered during collisions on a classical level. In the present work, the CTMC simulations were created using three-body approximation. In our CTMC model, the particles are the projectile (P), one atomic active target electron (e), and the remaining target ion (T), including the target nucleus and the remaining target electrons. Figure 1 shows the relative position vectors of the three-body collision system.

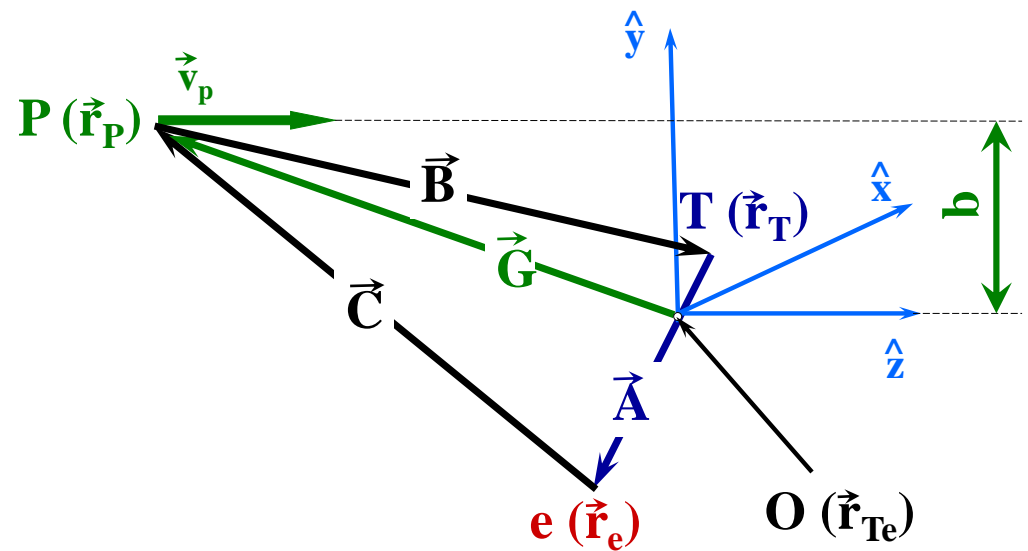


Figure 1. The relative position vectors of the particles involved in three-body collisions. $\vec{A} = \vec{r}_e - \vec{r}_T$, $\vec{B} = \vec{r}_T - \vec{r}_P$, and $\vec{C} = \vec{r}_P - \vec{r}_e, \vec{r}_{Te}$ are the relative position vectors, O (\vec{r}_{Te}) is the center of mass of the target system, \vec{G} is the distance between the projectile and the target system, and b is the impact parameter.

The particles were characterized by their masses (m_P, m_T , and m_e) and charges (Z_P, Z_T , and Z_e). In the case under consideration, $m_P = m_e$. We note that these models are classical analogues of the effective quantum-mechanical single-electron treatment of collisions in which the electrons are treated equivalently. In the CTMC model, the classical equations of motions were solved numerically [14–18]. For the description of the interaction between the active target electron and the target core, a central model potential developed by Green [19,20], which is based on the Hartree–Fock calculations, was used. The potential can be written as:

$$V(r) = q \frac{Z - (N - 1) \left(1 - \Omega^{-1}(r) \right)}{r} = q \frac{Z(r)}{r} \tag{1}$$

where Z is the nuclear charge, N is the total number of electrons in the atom or ion, r is the distance between the nucleus and the test charge q , and

$$\Omega(r) = \frac{\eta}{\xi}(e^{r\xi} - 1) + 1 \tag{2}$$

The potential parameters ξ and η can be obtained in such a way that they minimize the energy for a given atom or ion. We note that this type of potential has further advantages, because it has a correct asymptotic form for both small (Equation (3)) and large (Equation (4)) values of r .

$$\lim_{r \rightarrow 0} Z(r) = Z \tag{3}$$

$$\lim_{r \rightarrow \infty} Z(r) = Z - (N - 1) \tag{4}$$

The Lagrange equation for the three particles can be written as:

$$L = L_K - L_V \tag{5}$$

where

$$L_K = \frac{1}{2}m_P \dot{r}_P^2 + \frac{1}{2}m_e \dot{r}_e^2 + \frac{1}{2}m_T \dot{r}_T^2 \tag{6}$$

and

$$L_V = -\frac{Z_P \left(\frac{|\vec{C}|}{|\vec{C}|} \right) Z_e}{|\vec{C}|} + \frac{Z_P \left(\frac{|\vec{B}|}{|\vec{B}|} \right) Z_T \left(\frac{|\vec{B}|}{|\vec{B}|} \right)}{|\vec{B}|} + \frac{Z_e Z_T \left(\frac{|\vec{A}|}{|\vec{A}|} \right)}{|\vec{A}|} \tag{7}$$

$\vec{A} = \vec{r}_e - \vec{r}_T$, $\vec{B} = \vec{r}_T - \vec{r}_P$, and $\vec{C} = \vec{r}_P - \vec{r}_e$, \vec{r}_{Te} are the relative position vectors, and Z and m are the charge and the mass of the noted particle, respectively. Then, the equations of motion can be calculated as:

$$\frac{d}{dt} \frac{\partial L}{\partial \dot{q}_i} = \frac{\partial L}{\partial q_i}, \quad (i = P, e, T). \tag{8}$$

The equations of motion were integrated with respect to the time as independent variables using the standard Runge–Kutta method. For a given set of initial conditions the three-body, three-dimensional CTMC calculation was performed as described by Tőkési and Kövér [21]. After a large number of classical trajectory calculations, the total cross-section was computed using the following formula:

$$\sigma = \frac{2\pi b_{\max}}{T_N} \sum_j b_j^{(i)} \tag{9}$$

The statistical uncertainty of the cross-section is given as:

$$\Delta\sigma = \sigma \left(\frac{T_N - T_N^{(i)}}{T_N T_N^{(i)}} \right)^{1/2} \tag{10}$$

In Equations (9) and (10), T_N is the total number of trajectories calculated for impact parameters less than b_{\max} , $T_N^{(i)}$ is the number of trajectories that satisfy the criteria for ionization, and $b_j^{(i)}$ is the actual impact parameter for the trajectory corresponding to the ionization process.

3. Results and Discussion

A scaling rule for the electron impact cross-section maxima, σ_{\max} , for atomic systems was deduced in the following way. Initially, using experimental information available in the literature, a set of experimental cross-section maxima was tabulated for several atoms ranging from H to high Z species. Then, the dependences of the cross-sections on target polarizability, α , were methodically examined.

Upon categorizing the maximum cross-section data, we observed a noteworthy correlation of σ_{\max} with the target polarizability of the main group elements. This is shown in Table 1 and Figure 2 for several atomic species. The cross-section and polarizability data were obtained from several sources [2,5,22–36]. The electron impact and target polarizability data in Table 1 agree (within 10–30%) with other sources. We preferentially chose data from ref. [5] due to their accuracy (7%). The data clearly suggest that electron impact single-ionization cross-sections of atoms are bigger for atoms with larger dipole polarizability. Figure 2 shows linear dependence, with a fixed intercept, on the cross-sections with polarizability (Pearson’s R = 0.98796). By using a least-square fitting procedure and keeping the intercept fixed at zero, we found that the maximum cross-sections vary as follows: $\sigma_{\max}(\text{Mb}) = (132.9 \pm 4.5)\alpha(10^{-24} \text{ cm}^3)$. We also performed allometric fitting (see Table 2). However, linear fitting gives a slightly better result (larger R^2). Some systems do not follow the scaling, for instance, Mg (group 2), Fe (group 8), and Cu (group 11). The reasons are unknown at the moment.

Table 1. Polarizabilities [22–24] and electron impact single-ionization cross-section maxima [2,5,31,34,35] for atomic species. The data from ref. [5] present 7% accuracy and $\pm 10\%$ uncertainty.

Target	Polarizability (10^{-24} cm^3)	Cross-Section Maxima (Mb)	Reference
H	0.666	62.7	[2]
		73.0	[35]
He	0.20	37.5	[31]
		34.7	[36]
Ne	0.39	67.7	[36]
		73.5	[31]
Ar	1.64	255	[36]
		270	[31]
Kr	2.48	349	[36]
		370	[31]
Xe	4.04	467	[36]
		498	[31]
Al	6.8	978	[5]
Si	5.38	669	[5]
P	3.63	526	[5]
S	2.9	450	[5]
Ga	8.12	915	[5]
		1100	[34]
Ge	6.07	746	[5]
As	4.31	612	[5]
Se	3.77	590	[5]
In	5.35	832	[5]

Table 1. Cont.

Target	Polarizability (10^{-24} cm^3)	Cross-Section Maxima (Mb)	Reference
Sn	7.7	974	[5]
Sb	6.6	832	[5]
Te	5.5	826	[5]
Pb	6.8	832	[5]
Bi	7.4	876	[5]
O	0.802	136	[2]
		135.1	[35]
N	1.1	161.4	[2]
C	1.76	232.3	[2]
		227.3	[35]
Cl	2.14	349	[5]
B	3.05	400	[2]

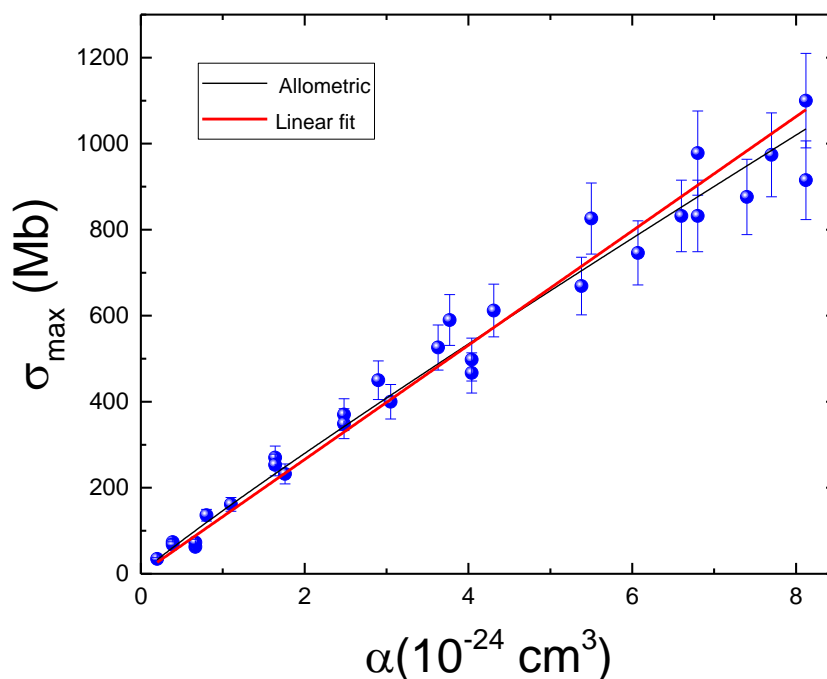


Figure 2. Electron impact single-ionization cross-section maxima of neutral atomic species as a function of target polarizability. The red line is a linear fitting ($\sigma_{\max} = a\alpha$). The black line is an allometric fitting ($\sigma_{\max} = b\alpha^a$). See Table 2 for the fitting parameters.

Table 2. Fitting parameters for Figure 2.

Equation	Parameter b	Parameter a	R ²
$Y = bx$	132.9 ± 4.5	-	0.97606
$Y = bx^a$	146.7 ± 6.9	0.933 ± 0.032	0.96302

This linear dependence suggests that the interaction potential between the projectile electron and the target electrons depends on the static polarizability, which leads to cross-section dependence that varies with static dipole polarizability. Langevin described the

square root dependence of a total-ionization cross-section with polarizability [27]. Polarizability is a measure of how promptly the target electronic charge distribution is disturbed by an external electric field. Among all the target electrons, valence electrons are those that contribute the most to the polarizability of atomic species. This suggests that the observed trend of cross-section maxima is a consequence of the importance of the most loosely bound valence electrons. For instance, some authors have calculated the maximum electron impact ionization cross-sections, σ_{\max} , for several atoms [24–28] using additive rules. They demonstrated that σ_{\max} is equal to contributions from the valence electrons weighted by the mean square radii of each shell. Target polarizability plays an important role not only in impact ionization, but also in polarization bremsstrahlung [27–30]. Dmitrieva and Plindov demonstrated that target polarizability, α , varies as follows: $\alpha \sim I_E^{-3}$, where I_E is the target ionization energy, which indicates how tightly bound the least bound electron is [29]. Thus, the electron impact cross-section σ should vary as follows: $\sigma \sim I_E^{-3}$.

To confirm our prediction, we performed CTMC calculations for some elements to obtain the electron impact ionization cross-sections. Figures 3 and 4 show our classical simulations results.

While Figure 3 shows the electron impact ionization cross-sections for hydrogen (^1H), helium (^4He), and neon (^{20}Ne) targets, Figure 4 shows the corresponding ionization cross-sections for argon (^{40}Ar), krypton (^{84}Kr), and xenon (^{131}Xe) targets in comparison with some previous representative experimental results. To reduce the statistical error of the cross-section calculations, we followed 500,000 individual random trajectories for each energy and each collision system.

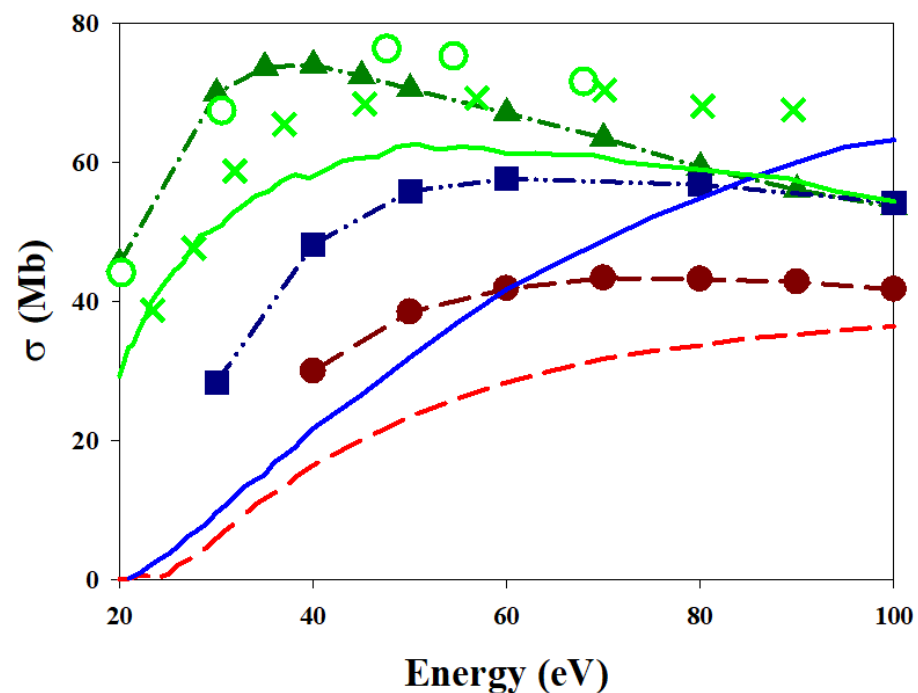


Figure 3. Electron impact single-ionization cross-section. Lines with symbols are our present CTMC results. Dark green dashed-dotted line with triangles: hydrogen target; dark red long-dashed line with circles: helium target; dark blue dashed-double-dotted line with squares: neon target. Experimental data: Solid green line: hydrogen target from Ref. [35]; open circles: hydrogen target from Ref. [33]; cross: hydrogen target from Ref. [34]; red dashed line: helium target from Ref. [36]; blue solid line: neon target from Ref. [36].

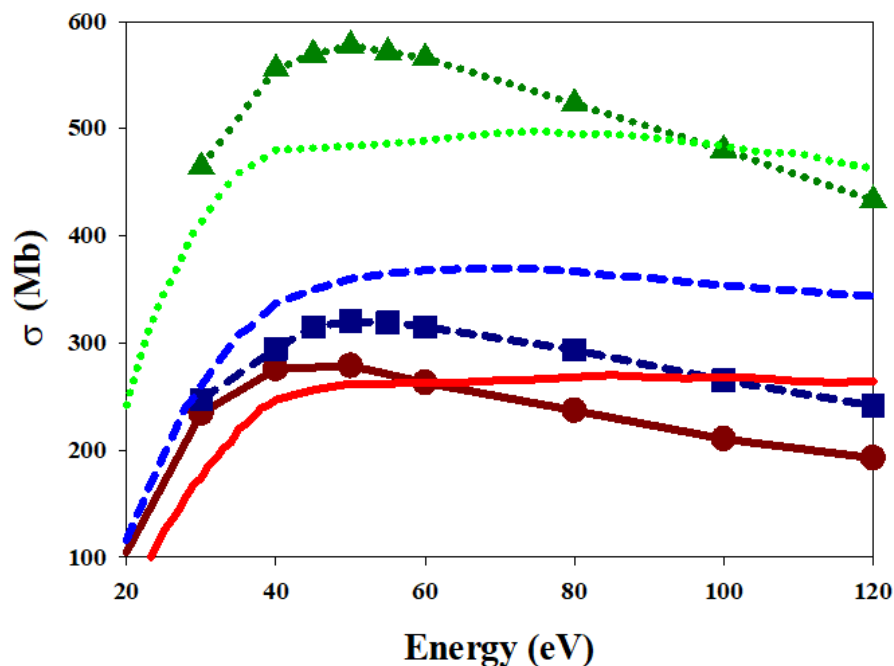


Figure 4. Electron impact single-ionization cross-section. Lines with symbols are our present CTMC results. Dark red long-dashed line with circles: argon target; dark blue dashed-double-dotted line: krypton target; dark green dotted line with triangles: xenon target. Experimental data: red solid line: argon target from Ref. [31]; blue dashed line: krypton target from Ref. [29]; dotted green line: xenon target from Ref. [31].

Figure 5 shows the experimental data, as well as the CTMC results of the electron impact single-ionization cross-section maxima of H, He, Ne, Ar, Kr, and Xe as a function of polarizability. We found good agreement between the theoretical data and the experimental observations, especially in lower nuclear charge states.

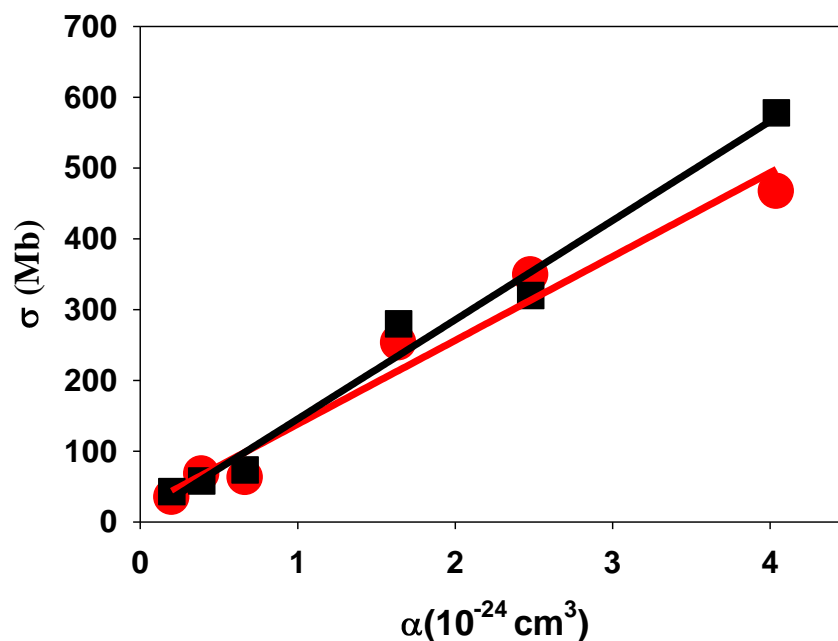


Figure 5. Electron impact single-ionization cross_section maxima of neutral atomic species as a function of polarizability. Red dots: experimental data; black squares: present CTMC results. The lines represent the linear fits through our data.

4. Summary

To summarize, the scaling behaviour of the electron impact single-ionization cross-section maxima, resulting from collisions with neutral atomic species, was obtained using experimental data obtained for an ample variety of targets. It was found that, in the case of single ionization, cross-sections scale linearly with ground state target dipole polarizability. We found that the maximum cross-sections vary as follows: $\sigma_{\max}(\text{Mb}) = (132.9 \pm 4.5)\alpha$ (10^{-24} cm^3), which may be useful for obtaining a rough estimation of electron impact single-ionization cross-sections for atomic species. Some elements do not follow the present linear fit, so scaling probably depends on the group in the periodic table. Our findings were verified using our CTMC calculations for noble gases.

Author Contributions: A.C.F.d.S.: collecting the data, writing the manuscript, and editing the results. K.T.: performing the simulations and writing the manuscript. All authors have read and agreed to the published version of the manuscript.

Funding: This work was supported by the CNPq (304404/2022-5), FINEP (0134/19), and FAPERJ (E-26/010-101116/2018).

Institutional Review Board Statement: Not applicable.

Informed Consent Statement: Not applicable.

Data Availability Statement: The data that support the findings of this study are available from the authors upon reasonable request.

Acknowledgments: A.C.F.S. acknowledges support from CNPq, CAPES, FINEP, and FAPERJ.

Conflicts of Interest: The authors declare no conflict of interest.

References

1. Inokuti, M. Inelastic Collisions of Fast Charged Particles with Atoms and Molecules—The Bethe Theory Revisited. *Rev. Mod. Phys.* **1971**, *43*, 297. [[CrossRef](#)]
2. Tawara, H.; Kato, T. Total and partial ionization cross sections of atoms and ions by electron impact. *At. Data Nucl. Data Tables* **1987**, *36*, 167–353. [[CrossRef](#)]
3. Deutsch, H.; Märk, T.D. Calculation of absolute electron impact ionization cross-section functions for single ionization of He, Ne, Ar, Kr, Xe, N and F. *Int. J. Mass. Spectr. Ion. Proc.* **1987**, *79*, R1–R8. [[CrossRef](#)]
4. Sorokin, A.A.; Shmaenok, L.A.; Bobashev, S.V.; Möbus, B.; Ulm, G. Measurements of electron-impact ionization cross sections of neon by comparison with photoionization. *Phys. Rev. A* **1998**, *58*, 2900. [[CrossRef](#)]
5. Freund, R.S.; Wetzel, R.C.; Shul, R.J.; Hayes, T.R. Cross-section measurements for electron-impact ionization of atoms. *Phys. Rev. A* **1990**, *41*, 3575. [[CrossRef](#)]
6. Almeida, D.P.; Fontes, A.C.; Godinho, C.F.L. Electron-impact ionization cross section of neon (σ_{n+} , $n = 1-5$). *J. Phys. B At. Mol. Opt. Phys.* **1995**, *28*, 3335. [[CrossRef](#)]
7. Almeida, D.P.; Fontes, A.C.; Godinho, C.F.; Matos, I.S. Electron impact multiple ionization cross section of argon (σ_{n+} , $n = 3-6$). *J. Electron Spectrosc. Relat. Phenom.* **1994**, *67*, 503–510. [[CrossRef](#)]
8. Almeida, D.P.; Fontes, A.C.; Pontes, F.C. Multiple ionization of gases by collisions with electrons. *Nucl. Instrum. Meth. Phys. Res. B* **1997**, *132*, 280–287. [[CrossRef](#)]
9. Bethe, H. Zur Theorie des Durchgangs schneller Korpuskular strahlen durch Materie. *Ann. Phys.* **1930**, *5*, 325. [[CrossRef](#)]
10. Otvos, J.W.; Stevenson, D.P. Cross-sections of Molecules for Ionization by Electrons. *J. Am. Chem. Soc.* **1956**, *78*, 546. [[CrossRef](#)]
11. Maiorov, S.A.; Golyatina, R.I. Analytical Formulas for Approximating Cross Sections of Electron Collisions with Hydrogen, Noble Gases, Alkali and Other Atoms. *Atoms* **2022**, *10*, 93. [[CrossRef](#)]
12. Tókési, K.; Hock, G. Versatility of the exit channels in the three-body CTMC method. *Nucl. Instrum. Meth. Phys. Res. B* **1994**, *86*, 201. [[CrossRef](#)]
13. Figueiredo, I.; Bundaleski, N.; Teodoro, O.M.N.D.; Jousten, K.; Illgen, C. Influence of ion induced secondary electron emission on the stability of ionisation vacuum gauges. *Vacuum* **2021**, *184*, 109907. [[CrossRef](#)]
14. Olson, R.E.; Reinhold, C.O.; Schultz, D.R. High-Energy Ion-Atom Collisions. In Proceedings of the IVth Workshop on High-Energy Ion-Atom Collision Processes, Debrecen, Hungary, 17–19 September 1990; Berényi, D., Hock, G., Eds.; Lecture Notes in Physics. Springer: Berlin/Heidelberg, Germany, 1991; Volume 376, p. 69.
15. Abrines, R.; Percival, I.C. Classical Theory of Charge Transfer and Ionization of Hydrogen Atoms by Protons. *Proc. Phys. Soc.* **1966**, *88*, 861. [[CrossRef](#)]
16. Olson, R.E.; Salop, A. Charge-transfer and impact-ionization cross sections for fully and partially stripped positive ions colliding with atomic hydrogen. *Phys. Rev. A* **1977**, *16*, 531. [[CrossRef](#)]

17. Tókési, K.; Hock, G. Angular distributions of low-energy electrons from proton-atom collisions. *Nucl. Instrum Meth. Phys. Res. B* **1997**, *124*, 398. [[CrossRef](#)]
18. Tókési, K.; Hock, G. Double electron capture in He²⁺ + He collisions up to 1500 keV/amu projectile impact. *J. Phys. B* **1996**, *29*, 119. [[CrossRef](#)]
19. Green, A.E.S. An Analytic Independent Particle Model for Atoms: I. Initial Studies. *Adv. Quantum Chem.* **1973**, *7*, 221–262.
20. Garvey, R.H.; Jackman, C.H.; Green, A.E.S. Independent-particle-model potentials for atoms and ions with $36 < Z \leq 54$ and a modified Thomas-Fermi atomic energy formula. *Phys. Rev. A* **1975**, *12*, 1144.
21. Tókési, K.; Kövér, Á. Electron capture to the continuum at 54.4 eV positron-argon atom collisions. *J. Phys. B* **2000**, *33*, 3067–3077. [[CrossRef](#)]
22. Lide, D.R. (Ed.) *Handbook of Chemistry and Physics*, 78th ed.; CRC: New York, NY, USA, 1997.
23. Fraga, S.; Karwowski, J.; Saxena, K.M.S. *Handbook of Atomic Data*; Elsevier Scientific Publishing Company: Amsterdam, The Netherlands, 1976.
24. Santos, A.C.F.; Almeida, D.P. On the shake-off probability for atomic systems. *J. Electron Spectrosc. Relat. Phenom.* **2016**, *210*, 1–4. [[CrossRef](#)]
25. Dmitrieva, I.K.; Plindov, G.I. Dipole Polarizability, Radius and Ionization Potential for Atomic Systems. *Phys. Scr.* **1983**, *27*, 402. [[CrossRef](#)]
26. Wetzell, R.C.; Baiocchi, F.A.; Hayes, T.R.; Freund, R.S. Absolute cross sections for electron-impact ionization of the rare-gas atoms by the fast-neutral-beam method. *Phys. Rev. A* **1987**, *35*, 559. [[CrossRef](#)] [[PubMed](#)]
27. Langevin, P. Une formule fondamentale de theorie cinetique. *Ann. Chem. Phys.* **1905**, *8*, 245.
28. Mann, J.B. Ionization Cross Sections of the Elements Calculated from Mean-Square Radii of Atomic Orbitals. *J. Chem. Phys.* **1967**, *46*, 1646. [[CrossRef](#)]
29. Tsyтович, V.N.; Oiringel, I.M. *Polarization Bremsstrahlung*; Translated from Russian; Plenum Press: New York, NY, USA, 1992.
30. Beilin, E.L.; Zon, B.A. On the sum rule for multiphoton bremsstrahlung. *J. Phys. B At. Mol. Phys.* **1983**, *16*, L159. [[CrossRef](#)]
31. Towari, P.; Kai, D.K.; Rusgi, M.L. Maximum Ionization Cross Section of Atoms. *J. Chem. Phys.* **1969**, *50*, 3040. [[CrossRef](#)]
32. Younger, S.M.; Mark, T.D. *Electron Impact Ionization*; Mark, T.D., Dunn, G.H., Eds.; Springer: New York, NY, USA; Berlin/Heidelberg, Germany, 1985.
33. Fite, W.L.; Brackmann, R.T. Collisions of electron with hydrogen atoms. I. Ionization. *Phys. Rev.* **1958**, *112*, 1141. [[CrossRef](#)]
34. Patton, C.J.; Lozhkin, K.O.; Shah, M.B.; Geddes, J.; Gilbody, H.B. Multiple ionization of gallium by electron impact. *J. Phys. B At. Mol. Opt. Phys.* **1996**, *29*, 1409–1417. [[CrossRef](#)]
35. Bell, K.L.; Gilbody, H.B.; Hughes, J.G.; Kingston, A.E.; Smith, F.J. Recommended Data on the Electron Impact Ionization of Light Atoms and Ions. *J. Phys. Chem. Ref. Data* **1983**, *12*, 891. [[CrossRef](#)]
36. Rejoub, R.; Lindsay, B.G.; Stebbings, R.F. Determination of the absolute partial and total cross sections for electron-impact ionization of the rare gases. *Phys. Rev. A* **2002**, *65*, 042713. [[CrossRef](#)]

Disclaimer/Publisher's Note: The statements, opinions and data contained in all publications are solely those of the individual author(s) and contributor(s) and not of MDPI and/or the editor(s). MDPI and/or the editor(s) disclaim responsibility for any injury to people or property resulting from any ideas, methods, instructions or products referred to in the content.